International Journal of Researches on Civil Engineering with Artificial Intelligence

www.ceai.reapress.com

Int. J. Res. Civ. Eng. AI. Vol. 1, No. 1 (2024) 21–39.

Paper Type: Original Article

Enhancing Concrete Performance with Waste Rubber: An Artificial Neural Network Approach for Mix Ratio Optimization and Predictive Analysis

Morteza Shariati[1,*] , Mohammad Habibi[2], Emad Toghroli[2], Maryam Ramezani[2]

[1] Department of Civil Engineering Discipline, School of Engineering, Monash University, Melbourne 3800, Australia; morteza_shariatee_sc@yahoo.com.

[2] Department of Civil Engineering, Calut Company Holding, Melbourne 3800, Australia; mohammad@calut.com.au; toghroli@calut.au; maryam.ramezani@sharif.edu

Citation:

Received: 01 February 2024 *Revised: 05 March 2024* *Accepted: 01 April 2024*	Shariati, M., Habibi, M., Toghroli, E., & Ramezani, M. (2024). Enhancing concrete performance with waste rubber: an artificial neural network approach for mix ratio optimization and predictive analysis. *International journal of researches on civil engineering with artificial intelligence, 1* (1), 21-39.

Abstract

Due to its enhanced mechanical qualities and environmental sustainability, waste rubber in concrete materials has attracted more attention. In this investigation, a numerical model was suggested to clarify the effect of rubber tiering on strengths. Given the variety of raw materials available then, changing how concrete works to fit modern development is hard. The standard mixing ratio test method could be replaced with the artificial neural optimization model, and the concrete performance prediction could be realized accurately and quickly. This will allow for the more efficient use of a wide range of complex novel raw materials and improve the concrete mix ratio design method. Evaluating the workability, compressive, splitting, tensile, and bending strengths include replacing rubber waste particles with 10%, 20%, and 30% of aggregates by volume. Data was collected from the literature, and the results were analyzed using an Extreme Learning Machine (ELM) and Multiple Linear Regression (MLR) to accurately evaluate rubberized concrete beams' performance with micro-reinforcement. The results revealed that using rubber waste particles leads to a decline in the weight of the concrete sample and a level of Compressive Strength (CS) compatible with a load-bearing wall. The regression analysis revealed a high correlation between the independent and dependent variables, with R^2 values ranging from 0.932 to 0.983 in both the training and testing phases. However, there was higher variability in the test phase, with RSD values ranging from 6.23% to 9.92%, compared to the training phase, with RSD values ranging from 5.12% to 6.77%. The study demonstrated the potential to use waste rubber in concrete composites and the importance of considering the training and test phase results for accurate predictions. Regarding accuracy, both models have relatively high R^2 values (0.954 for ELM and 0.943 for MLR), indicating a strong correlation between the independent and dependent variables. However, ELM has a slightly lower RSD (6.88%) than MLR (5.45%). Regarding Mean Relative Error (MRE), both models have similar results (5.12% for ELM and 5.87% for MLR). In terms of time, the ELM model has a much faster running time of 2.45 seconds compared to the MLR model, which takes 28.011 seconds. ELM can make predictions faster than MLR, which could be significant in real-time applications.

Keywords: Concrete, Waste rubber tier, Multiple linear regression, Extreme learning machine.

Corresponding Author: morteza_shariatee_sc@yahoo.com.a@

1 | Introduction

Modifying building materials to achieve the desired features, sustainability, and economy is a major concern for the sector. Waste materials, such as fly ash, glass fibers, and tire rubber, among others, are always preferred for construction because they are affordable and reduce disposal issues. Concrete is the most common building material, but it uses the most natural resources. Water, cement, and aggregate [1]-[3] hold it together. Unless a replacement can be discovered, using traditional materials in concrete will exhaust the resources. Due to its properties, rubber can be a suitable replacement for good aggregates in concrete structures. Vehicle use increased in tandem with global population growth. As a consequence, the annual production of rubber reached its highest level. As a result, burning it or dumping it in landfills is the quickest and cheapest way to dispose of used tire rubber [4]. However, burning results in global warming, toxic emissions, and smoke pollution, all of which are dangerous to human health and other ecosystems [5]-[7]. If used rubber tires are disposed of in sanitary landfills, additional problems arise, such as contamination and environmental risks. Waste tires aren't allowed to be thrown away in some countries due to their weight, their tendency to flow on the ground, and other things that could be harmful. For this reason, waste rubber recycling has been promoted worldwide, regardless of environmental or economic concerns [8]. Using it as an additive in concrete-based products is the most efficient way to dispose of these non-decomposing rubber materials. Rubber is often used in engineering structures since it has several benefits and has a massive effect on the durability and strength characteristics of reinforced concrete structures. It can be used to build steel-concrete composite beams, rigid pavements, airport pavements, and earthquake-resistant structures. Using waste rubber in the mix enhances Concrete's energy absorption, strain capacity, crack resistance for microcracking, impact resistance, and fracture toughness. Rubber can be added to the concrete to decrease its tendency to fracture easily. Rubberized concrete shows plastic failure modes and ductile behavior. Crumb rubber provided better blast and explosion resistance. Unlike normal concrete, rubberized concrete has an appealing look, a usable texture, and a lower unit weight [9]-[11]. The behavior of concrete incorporating rubber waste has been the subject of several studies in the past. For example, Khatib and Bayomy [12] studied how the slump of rubber concrete changes and found that the slump decreases with an increasing percentage of rubber. According to another report, there was no slump when the rubber content exceeded 40%. More mixtures with fine rubber particles were workable than coarser ones [12]. According to Fedroff et al. [13], adding rubber particles increased air volume in the mix [14]. Compared to smaller rubber aggregates and coarse aggregates, the loss of CS was less. Rubber has a high absorption capacity; therefore, it failed ductility when rubberized concrete was pressed [14]. Blastomeres, other materials, and 3.5% to 5% of rubber were used by Hernandez-Olivares et al. [15]. They performed many tests and concluded that the CS of rubber plastic was 23 MPa, compared to 36 MPa for their control mixture [15]. Shu and Huang [16] concluded that rubber concrete has weaker properties overall than normal concrete. Based on the results, rubber particles of larger sizes in concrete mixtures had lower strength than smaller ones [17]-[19]. There is a huge potential for waste rubber reuse and recycling in developing countries due to the enormous amount of waste tire rubber. Reduced waste and less environmental deterioration arise from reusing, recycling, or handcrafting rubber tires into new products [20]. Two different technologies were obtained for rubber aggregate from the waste tire (mechanical grinding and cryogenic grinding) [21]. The high ductility, crack resistance, and strong energy dissipation capacity have been achieved by introducing a certain amount of crumb rubber in normal concrete, known as crumb rubber concrete [22]. The Compressive Strength (CS) and density of rubberized concrete are affected by the rubber content and w/c ratio [23]. The bonding strength of rubber aggregates can be increased by treating it with carboxylic acids and styrene-butadiene copolymer latex admixtures [24], [25]. The CS of cementitious materials has recently been forecast by different studies using extrapolation methods, Artificial Neural Networks (ANNs), compressible packing models, genetic algorithms, regression analysis methods, and fuzzy logic [26], [27]. According to its capacity to learn from output and input connections in complex issues, the ANN, among these approaches, seems to be a relevant and efficient approach [28]. In addition, ANN may be applied to map the mechanical properties of concrete, including its slumping, filling capacity, segregation, and CS and tensile strengths [26]-[28]. According to studies published in recent years, ANNs can be applied

to solve engineering problems. However, the data required [29] to evaluate the CS of concrete may be difficult to find or insufficient. These studies examined self-compacting [30]-[33], high performance [34]-[40], sulfate resistance [41], [42], lightweight [43]-[45], recycled aggregate [34], [46], [47], cyclic behavior of concretes [48] and waste material [41], [49], [50] issues. In 2021, more than 10,150 papers were published just in the field of materials engineering. This shows that machine learning and artificial intelligence are becoming increasingly popular. Faridehmihr et al. [51] investigated the use of waste materials in alkali-activated materials, including waste ceramic powder, palm oil, fly ash, and granulated blast-furnace slag. A meta-heuristic Krill-Herd algorithm and an ANN can be used to accurately predict properties like mechanical resistance [52]-[58]. In their investigation of the ternary blended alkali-activated mortars' cradle-to-gate life-cycle evaluation, Faridehmihr et al. [51] displayed the efficacy of ANNs. Mhaya et al. [59] tested the efficiency of several modified rubberized concretes by putting them in harsh environments. The final mechanical features were predicted using ANN and particle swarm optimization (PSO). In similar research, Golafshani and Behnood [60] used a multi-objective multi-verse optimizer with an ANN (PSO) and ANN (MOMVO). Alabduljabbar et al. [61] used a method similar to Sadowski et al. [62] to figure out the mechanical features of a large empirical study on the sustainability of using waste sawdust and complementary cementitious material to make high-efficiency, cement-free lightweight concrete. Ray et al. [63] used an ANN to examine how adding condensate milk and fine glass aggregate can fiber (Sn) changed the CS and splitting tensile strengths at three curing ages. The findings indicated that the accuracy was very good. It is obvious that by using machine learning technology, concrete value predictions may be made effectively [64], [65]. *Fig. 1* shows the Rubber tier waste recycling.

Fig. 1. Rubber-tier waste recycling.

Several works have examined how to make numerical models showing rubberised concrete's behaviour [66]-[68]. Topçu and Sardemir [69] used ANNs to predict rubberized concrete density and usage. Using the same technique, Bachir et al. [70] estimated the CS of rubberized concrete. To measure the CS of rubberized concrete, Jalal et al. [71] and Jalal and Jalal [72] highlighted the abilities of genetic programming, support vector machines, adaptive fuzzy neurosis inference systems, and multivariable non-linear and linear regression. Cheng and Cao [73] applied similar methods to measure the TS of rubberized concrete. Habib and Yildirimused [74] multivariable linear regression to estimate rubberised concrete's dynamic features. As a result, multivariable regression analysis, which is easy to use, deals with a few independent parameters whose values are to measure a single outcome variable [75]. For estimating rubberized concrete characteristics, a

neural network is more precise but more intricate and rarely used by practicing engineers [74].

The primary indicator, the CS of SCRC, which is commonly used to assess strength, generally decreases as the rubber content of SCRC increases. Building codes like Eurocode 2 [76] or ACI Committee 209 have no expressions for predicting the CS of rubberized concrete, especially SCRC. This demonstrates that a concrete reference mixture devoid of crumb rubber particles is always required. As a result, one of several machine learning methods was used in their article to attempt to forecast the CS of SCRC. Various fields, especially process control and optimization, medicine, engineering, and economics, have successfully used metaheuristic methods, especially neural networks [76]-[80]. They have also been used to imitate how the material behaves when it is fresh or solid [62], [81]-[84], though this is much less true in concrete that has been strengthened with rubber [85]-[87]. In addition to ANN models, the CS of concrete has also been estimated using Random

Forest and K-Nearest Neighbor (KNN), two other methods for machine learning [89]. KNN uses the distances of the k-nearest data points to assign unknown data values.

On the other hand, the ensemble learning method RF produces many decision trees during training. RF gives unknown data values depending on the mean forecast of the individual trees. With 104 experimental data points, Ahmadi-Nedushan [90] used a KNN to forecast the CS, while Chopra et al. [91] used an RF model and 49 data points to estimate the CS. *Fig. 2* shows the process of converting waste rubber to graphene, which involves heating the rubber to high temperatures in an oxygen-free environment, resulting in carbon atoms rearranging into graphene sheets. This process is known as thermal decomposition or pyrolysis. The graphene sheets are then collected and purified for use in various applications.

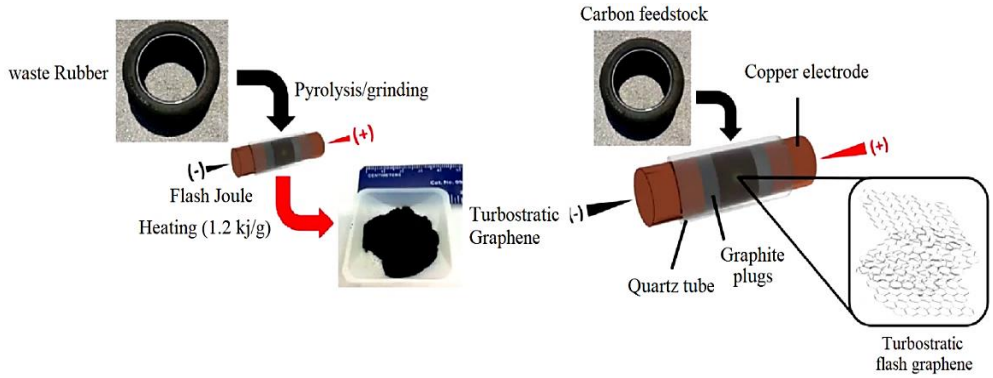

Fig. 2. Converting waste rubber to graphene.

1.1 | Problem Statement-Objective of Study

Rubberized concrete is an eco-friendly material with superior vibration behavior and energy dissipation capabilities; therefore, the research on it has expanded considerably over the last decade. Despite this, a number of investigations have shown that the presence of rubber in a material reduces its mechanical properties. These models are more complex than multivariable regression models and take more computational effort in engineering practice. In addition, the bulk of research has concentrated only on the CS of rubberized concrete and has seldom looked into other characteristics and sample sizes. This project seeks to produce simple and accurate multivariable linear regression models for rubberized concrete and an Extreme Learning Machine (ELM) that can be applied to various rubberized concrete compositions and sample sizes. The research aimed to explore the use of scrap rubber in concrete composites and its influence on the composites' strengths. Data was acquired from the literature and analyzed using MLR and ELM to assess the performance of rubberized concrete beams with micro-reinforcement.

1.2 | Significance of Study

This study's significance lies in exploring the potential of waste rubber in concrete composites as a sustainable building material. The numerical model proposed helps gain insights into the effect of rubber tires on concrete strengths. Using intelligent optimization algorithms to design the concrete mix ratio and predict concrete performance helps efficiently use diverse raw materials. The study's results showed the compatibility of rubber waste particles in reducing the weight of the concrete sample while maintaining a level of CS. The comparison of MLR and ELM models showed that both models have high accuracy, but ELM has a faster running time, which could be significant in real-time applications. *Fig. 3* shows the application of rubber bricks. *Fig. 4* shows the shredding line: the process starts with removing the steel wire from the tire, followed by shredding the tire into smaller pieces. The shredded rubber is then processed further to remove impurities and produce rubber granules or powders for various applications. The tire shredding line improves the efficiency and sustainability of the tire recycling process.

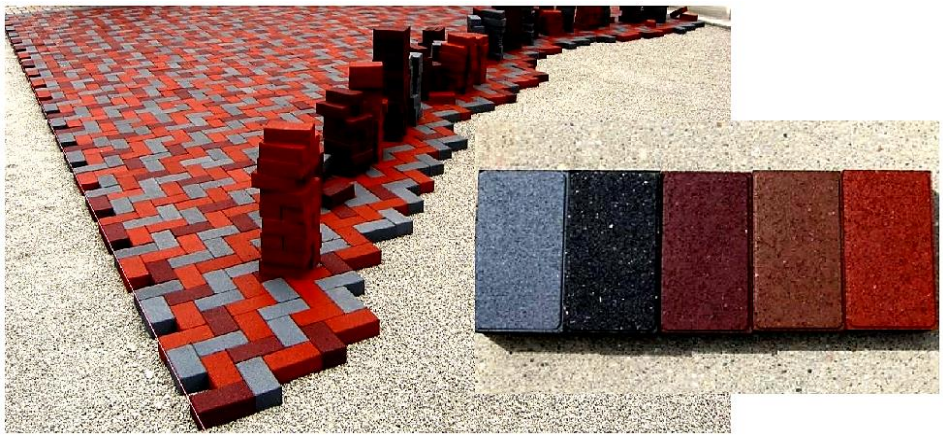

Fig. 3. Rubber tier bricks.

2 | Methodology

2.1 | Materials

This study prepared a concrete mix by replacing fine aggregates with different percentages of waste rubber particles: 10%, 20%, and 30%. The workability, TS, CS, and Bending Strengths (BSs) s of the concrete were evaluated and compared with traditional concrete. The experiments were conducted following the standard procedures, and the results were analyzed using MLR and ELM models to evaluate the efficiency of rubberized concrete beams with micro-reinforcement. The study investigated the potential of using waste rubber in concrete composites and the importance of considering the results for accurate predictions. The mix proportions of rubber fiber concrete used in this study were cement (150 kg/M^3), coarse aggregate (600 kg/M^3), rubber particles (A1 (0.6 kg/m^3), A2 (0.9 kg/m^3), A3 (1.5 kg/m^3)), fine aggregate (450 kg/M^3), fly ash (10, 20, or 40) orders as per study requirement Polypropylene fiber (0.75 kg/M^3), admixture (1.5%) of the total cement weight.

Table 1. A mix ratio of rubber fiber concrete was used in the study.

Material	Amount (kg/m^3)
Cement	150
Coarse aggregate	600
Rubber particles	0.6, 0.9, 1.5
Fine aggregate	450
Fly ash	10, 20, or 40 (as per study requirement)
Polypropylene fiber	0.75
Admixture	1.5% of total cement weight

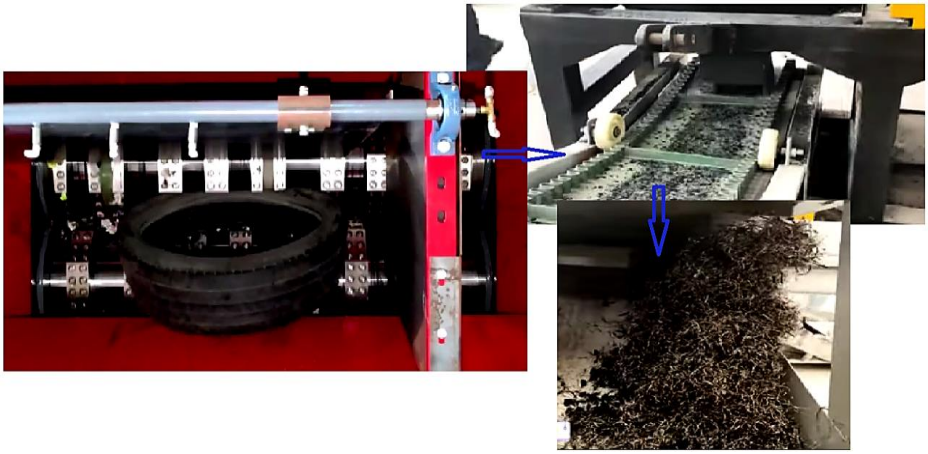

Fig. 4. Rubber tier shredding line.

2.2 | ELM Development

ELM is a functional programming language that compiles JavaScript and is used for building web applications, as reported by Huang et al. [92], [93]. It was created by Evan Czaplicki in 2012 as part of his thesis project at Harvard University. ELM is designed to make creating reliable and maintainable web applications easier by providing a strong type system, a clear separation of concerns, and a focus on immutability. One of the main benefits of using ELM for web development is its focus on functional programming. This approach can make it easier to reason about the behavior of your application and to write code that is easier to test and maintain. ELM's type system is another key feature that makes it popular for web development [93]-[96]. The type system helps catch errors at compile time rather than at runtime. This means many bugs can be caught early in development, reducing debugging time. ELM also provides a clear separation of concerns through its architecture pattern, the ELM architecture. The ELM architecture promotes separation between the model, the view, and the update function, making it easier to reason about the behavior of your application and to write code that is easier to maintain and modify.

Regarding development, ELM provides a range of tools and resources to make it easier to build web applications. For example, ELM has a package manager, which makes it easy to use external libraries and dependencies in your ELM projects. There is also an interactive environment called the ELM REPL, which allows you to experiment with ELM code and learn about the language's syntax. ELM is a popular choice for web development, particularly for those interested in functional programming who want to build reliable and maintainable web applications. Its focus on immutability, strong type system, and clear separation of concerns make it an attractive option for developers who want to build high-quality web applications [95].

$$\sum_{i=1}^{M} Q, \Omega\left(x_j\right) = \sum_{i=1}^{M} Q, \Omega\left(x_j, c_i + d_i\right) = \tau_i, j = 1, \dots, N, \quad (1)$$

where $c_i = \left[c_{ii}, c_{i_2} \dots, c_{i+1}\right]^T$ is the weight vector that is randomly built to connect the i th hidden nodes of the hidden layer and input nodes, $Q = [Q_a, Q_{ia}, \dots, Q_{im}]^T$ is the output weight vector connecting hidden nodes and output nodes, and d_i is the bias of the i th hidden node. x_p, c_i denotes the inner product of x_j and c_i. The output of the ith hidden node with respect to the input sample x_j is $\Omega\left(x_j, c_i + d_j\right)$[95].

$$KQ = T, \quad (2)$$

where

$$K = \begin{bmatrix} \Omega(x_1, c_1 + d_1) & \cdots & \Omega(x_1, c_M + d_M) \\ \vdots & \ddots & \vdots \\ \Omega(x_N, c_1 + d_1) & \cdots & \Omega(x_N, c_M + d_M) \end{bmatrix}_{NWM},$$
$$Q = \begin{bmatrix} Q_1 \\ Q_2 \\ \vdots \\ Q_M \end{bmatrix}_{M\times 1} \quad \text{and} \quad T = \begin{bmatrix} t_1 \\ t_2 \\ \vdots \\ t_N \end{bmatrix}_{N\times 1}. \tag{3}$$

K is termed the hidden layer output matrix of the single-layer feedforward NN. The ith column of *K* shows the *i* th node in the hidden layer in terms of inputs $x_1, x_2, \dots, x_{\mathbb{N}^*}\Omega(x_1, c_1 + d_1)$ is named the hidden layer feature mapping [93].

$$\|K(c_1, \dots, c_N, d_1, \dots, d_N)Q - T\| = \min_{c,b,4} \|K(c_1, \dots, c_N, d_1, \dots, d_N)Q - T\|. \tag{4}$$

Eq. (3) corresponds to the reduction of the cost function.

$$E = \sum_{j=1}^{N} \left(\sum_{i=1}^{M} Q\Omega(x_i, c_i, d_i) - \tau_j \right)^2. \tag{5}$$

According to the theories underlying the ELM, almost all non-linear functions similar to those applied in feature mappings could be used to provide universal approximation in the ELM [98].

$$\left\| K\hat{Q} - T \right\| = \left\| KKT - T \right\| = \min_{Q} \left\| KQ - T \right\|. \tag{6}$$

Table 2. Steps involved in the preparation of rubber fiber concrete.

Step	Process
1	Mixing of dry ingredients: the fine aggregate, cement, coarse aggregate, fly ash, and rubber particles were mixed in a dry state in a laboratory mixer.
2	Addition of admixture: the polycarboxylic acid superplasticizer was added to the mixture and thoroughly mixed for 1 minute.
3	Addition of water: water was added to the mixture, and the mixing was continued for another 5 minutes.
4	Addition of fiber: polypropylene fiber was added to the mixture, and the mixing was continued for a final 1 minute.
5	Molding of specimens: the prepared mixture was then cast into cube, cylinder, and beam specimens of standard dimensions and cured under laboratory conditions.
6	Testing of specimens: After curing, the specimens were tested for CS, TS, and BSs per relevant standards.

2.3 | MLR Development

In engineering, MLR is commonly used to predict the response of a system based on the values of multiple input variables. For example, in the field of mechanical engineering, MLR can be used to predict the strength of materials based on their chemical composition and manufacturing processes. In civil engineering, MLR can be used to estimate the CS of concrete based on its ingredients and curing time. In electrical engineering, MLR could be applied to forecast the performance of electrical devices based on their design parameters. In general, MLR is a useful tool for solving linear problems in engineering where there is a relationship between multiple independent variables and a dependent variable that can be modeled using a linear equation (*Fig. 5*).

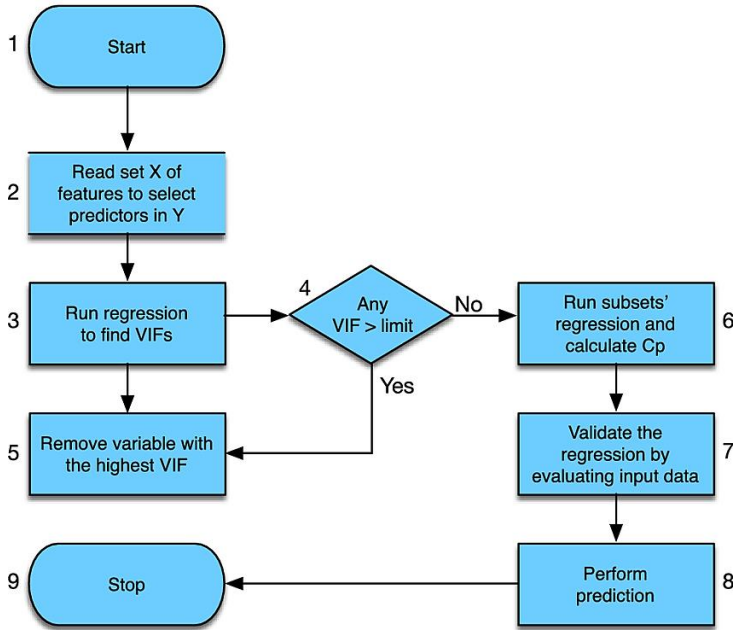

Fig. 5. MLR flowchart [99].

2.4 | Interpretation of the Test Results Using Statistical

The mechanical functions of TS (f_{st}), CS (f_c), impact energy (E_F), and flexural strength (f_f) were assessed using steel fiber (0, 0.75, 1.15, and 1.55%) and Multiple Linear Regression (MLR) analysis on fly ash (0 and 40%). The regression analysis's equation is expressed as

$$Y = \beta_0 + \beta_1 X_1 + \beta_2 X_2 + \varepsilon. \quad (7)$$

Y is the dependent variable that needs to be identified, X_i are the independent variables; β_i is the parameters; and ε are the errors. Final impact energy (E_F), flexural strength (f_f), CS (f_c), and split tensile strength (f_{st}) were considered to be the dependent parameters to be defined from the known independent parameters (% of fly ash, X_1 and percentage of steel fibers, X_2) added to the mix. Based on *Eq. (2)*, statistical equations based on the experimental findings at 28 and 56 days were suggested. The regression parameters for the respective strength or energy at 28 or 56 days are symbolized by β_i in the equations below. It is suggested that the equations be used to predict the split tensile strength (f_{st}), CS (f_c), impact energy (E_F), and flexural strength (f_f) at 28 days.

$$f_c(\text{MPa}) = \beta_{(c-28)n} + \beta_{(c-2))1} X_1 + \beta_{(c-28)2} X_2, R^2 = 0.971. \quad (8)$$

The concrete used as the control had a CS of $\beta_{(c-28)0} = 98.53\%$; $\beta_{(c-28)1} = -0.131$; $\beta_{(c-28)2} = +4.295$.

$$f_{sr}(\text{MPa}) = \beta_{(-28)0} + \beta_{(t-28)1} X_1 + \beta_{(t-28)2} X_2, R^2 = 0.937. \quad (9)$$

The concrete used as the control had a split tensile strength of $\beta_{(t.28)0} = 101.42\%$; $\beta_{(t-28)1} = -0.013$; $\beta_{(c-28)2} = +0.860$.

$$f_f(\text{MPa}) = \beta_{(\gamma-28,0} + \beta_{(f-2)|1} X_1 + \beta_{(J-28)^2} X_2, R^2 = 0.955. \quad (10)$$

The concrete used as the control had a flexural strength of $\beta_{(f.28)0} = 100.81\%$; $\beta_{(f.28)1} = -0.028$; $\beta_{(f.28)2} = +1.584$.

$$E_F(\text{kN} - \text{mm}) = \beta_{(E-28)0} + \beta_{(E-28)1} X_1 + \beta_{(E-28)2} X_2, R^2 = 0.964. \quad (11)$$

The concrete used as the control had a final impact on the energy of $\beta_{(E-28)0} = 111.62\%$; $\beta_{(E-28)1} = -14.287$; $\beta_{(E-28)2} = +945.35$.

Based on the following equations, at 56 days, split tensile strength (f_{st}), CS (f_c), impact energy (E_F), and flexural strength (f_f) can all be predicted:

$$f_c(\text{MPa}) = \beta_{(c-56)0} + \beta_{(c-56)1}X_1 + \beta_{(c-56)2}X_2, R^2 = 0.974. \quad \textbf{(12)}$$

The concrete used as the control had a CS of $\beta_{(c-56)0} = 100.82\%$; $\beta_{(c-56)1} = -0.064$; $\beta_{(c-56)2} = +5.698$.

$$f_{st}(\text{MPa}) = \beta_{(t-56)0} + \beta_{(t-56)1}X_1 + \beta_{(t-56)2}X_2, R^2 = 0.950. \quad \textbf{(13)}$$

The concrete used as the control had a split tensile strength of $\beta_{(t-56)0} = 97.84\%$; $\beta_{(t-56)1} = -0.013$; $\beta_{(c-56)2} = +0.864$.

$$f_f(\text{MPa}) = \beta_{g-56j0} + \beta_{(f-56)1}X_1 + \beta_{(f-56)2}X_2, R^2 = 0.939. \quad \textbf{(14)}$$

The concrete used as the control had a flexural strength of $\beta_{(f556)0} = 110.44\%$; $\beta_{(f.56)1} = -0.030$; $\beta_{(f.56)2} = +1.646$.

$$E_F(\text{kN} - \text{mm}) = \beta_{(E-56))} + \beta_{(E-56)]}X_1 + \beta_{(E-56)2}X_2, R^2 = 0.981. \quad \textbf{(15)}$$

The concrete used as the control had a final impact on the energy of $\beta_{(E-56)0} = 103.79\%$; $\beta_{(E-56)1} = -16.378$; $\beta_{(E-56)^2} = +1130.757$.

Based on a 95% confidence interval, *Eqs. (3)-(10)* are constructed. This shows that the error is very minimal and may be neglected because the regression coefficient (R^2) varies from 0.9 to 1 [100].

$$y = \beta_0 + \beta_1 x_1 + \beta_2 x_2 + \cdots + \beta_k x_k + \epsilon, \quad \textbf{(16)}$$

where

- y : response, $x_1, \ldots, x_k$: predictors.
- $\beta_0, \beta_1, \ldots, \beta_k$: coefficients.

ϵ : error term.

$$y = \begin{bmatrix} y_1 \\ y_2 \\ \vdots \\ y_n \end{bmatrix}, X = \begin{bmatrix} 1 & x_{11} & x_{12} & \cdots & x_{1k} \\ 1 & x_{21} & x_{22} & \cdots & x_{2k} \\ \vdots & \vdots & \vdots & \ddots & \vdots \\ 1 & x_{n1} & x_{n2} & \cdots & x_{nk} \end{bmatrix}, \beta = \begin{bmatrix} \beta_0 \\ \beta_1 \\ \vdots \\ \beta_k \end{bmatrix}, \epsilon = \begin{bmatrix} \epsilon_1 \\ \epsilon_2 \\ \vdots \\ \epsilon_n \end{bmatrix}. \quad \textbf{(17)}$$

Remark: This is the same formula for $\hat{\beta} = \left(\hat{\beta}_0, \hat{\beta}_1\right)'$ in simple linear regression. To show it, consider the following toy data set of three points: (0,1), (1,0), (2,2) used before. The new formula gives that

$$\begin{aligned} \hat{\beta} &= (X'X)^{-1}X'y \\ &= \left(\begin{bmatrix} 1 & 1 & 1 \\ 0 & 1 & 2 \end{bmatrix}\begin{bmatrix} 1 & 0 \\ 1 & 1 \\ 1 & 2 \end{bmatrix}\right)^{-1}\begin{bmatrix} 1 & 1 & 1 \\ 0 & 1 & 2 \end{bmatrix}\begin{bmatrix} 1 \\ 0 \\ 2 \end{bmatrix} \\ &= \begin{bmatrix} 3 & 3 \\ 3 & 5 \end{bmatrix}^{-1}\begin{bmatrix} 3 \\ 4 \end{bmatrix} \\ &= \begin{bmatrix} 0.5 \\ 0.5 \end{bmatrix}. \end{aligned} \quad \textbf{(18)}$$

3 | Result and Discussion

This study prepared rubber fiber concrete by replacing fine aggregates with different percentages of waste rubber particles: 10%, 20%, and 30%. The bending, TS, and CSs of the concrete were evaluated. The mixture ratio of the rubber fiber concrete used in this work was 150 kg/m^3 of fly ash, 450 kg/m^3 of cement, 600 kg/m^3 of fine aggregate, 800 kg/m^3 of coarse aggregate, 0.6, 0.9, 1.5 of rubber particles, 0.75 kg/m^3 of polypropylene fiber, and 1.5% of the total cement weight of polycarboxylic acid superplasticizer. The preparation of rubber fiber concrete involved mixing dry ingredients, including cement, coarse aggregate, fly ash, fine aggregate, and rubber particles, in a laboratory mixer. The polycarboxylic acid superplasticizer was then added and mixed for 1 minute, followed by the addition of water and mixing for another 5 minutes.

3.1 | Bending Strength

Following *Table 3*, the analysis of the given information highlights the importance of considering different parameters while using rubber tires in concrete. The rubber tire ratios play a crucial role in determining the strength of the concrete. Among the three ratios given (A1: 0.6 kg/m^3, A2: 0.9, A3: 1.5), A1 has the highest CS (33.40), while A3 has the lowest (28.10). However, when it comes to BS, A1 (5.15) has the lowest value compared to A2 (4.60) and A3 (4.29). The tensile strength of A1 (2.89) is also lower compared to A2 (2.50) and A3 (2.20). The addition of fly ash also impacts the strength of the concrete. The results show that the highest strength was observed at a fly ash dosage of 40 orders. This indicates that the proper addition of fly ash can significantly enhance the strength of the concrete. The test amounts of other materials, such as coarse aggregate, cement, polypropylene fiber, fine aggregate, and admixture, also play an important role in determining the strength of the concrete. An optimized combination of these materials is necessary to achieve the desired strength. Calculating the F factor quantitatively measures each parameter's relative importance on the concrete's overall strength. The results show that the CS has the highest contribution (38.70) to the F factor, followed by BS (0.720) and tensile strength (0.320). This emphasizes the significance of high CS when using rubber tires in concrete. Comparing concrete with diverse particle sizes of rubber reveals the impact of particle size on the mechanical properties of rubberized concrete. The compression strength of concrete with 0.6 kg/m^3 rubber particles was higher compared to concrete with 0.9 kg/m^3 rubber particles, with a compression strength increase of approximately 22%. The same trend was observed in the BS, where the concrete with 0.6 kg/m^3 rubber particles had a higher value than concrete with 0.9 kg/m^3 rubber particles, with a BS increase of approximately 8%. The tensile strength of concrete with 0.6 kg/m^3 rubber particles was also higher compared to concrete with 0.9 kg/m^3 rubber particles, with a tensile strength increase of approximately 14%. This indicates that smaller rubber particles contribute to higher strength in rubberized concrete.

Table 3. Strength characteristics of rubber tires in concrete: results and analysis.

Parameter	A1 (0.6 kg/ m^3)	A2 (0.9)	A3 (1.5)	Freedom	F Factor
Compressive Strength (CS)	33.40	31.52	28.10	2	38.70
Bending Strength (BS)	5.15	4.60	4.29	2	0.720
Tensile Strength (TS)	2.89	2.50	2.20	2	0.320

Based on *Table 4*, the mix for construction contains cement (150 kg/m^3), coarse aggregate (600 kg/m^3), rubber particles (0.6, 0.9, 1.5 kg/m^3), fine aggregate (450 kg/m^3), fly ash (10-40 kg/m^3), polypropylene fiber (0.75 kg/m^3), and 1.5% admixture. The test results show that the materials used in the mix have high strength, as evidenced by the R2 values in the CS test of 0.939, the TS test of 0.932, and the BS test of 0.934. These values show a strong relationship between the predictor and response variables. The Relative Standard Deviation (RSD) values in the CS test are 8.73%, in the tensile strength test are 6.23%, and in the BS test are 9.92%. These values represent the degree of variability or dispersion in the results of each test, with lower RSD values indicating lower variability and higher accuracy in the results. The RSD values for CS, TS, and BS are lower than the R2 values obtained from the same tests, suggesting good accuracy and consistency in the results. The Mean Relative Error (MRE) values in the CS test are 6.55%, in the tensile strength test are 5.23%, and in the

BS test are 7.77%. These values represent the average difference between the measured and actual values, with lower MRE values indicating higher accuracy in the results. The MRE values for CS, TS, and BS are within acceptable limits, supporting the conclusion that the mix is well-suited for construction applications.

Table 4. Comparing the strengths of the MLR model.

Dataset		R^2	RSD%	MRE%
Compressive strengths	Training	0.983	5.16	3.65
	Testing	0.939	8.73	6.55
Tensile strengths	Training	0.955	6.77	4.19
	Testing	0.932	6.23	5.23
Bending strengths	Training	0.945	5.12	4.33
	Testing	0.934	9.92	7.77

3.2 | Prediction Compressive Strength

Following *Table 5*, the need for faster progress on any infrastructure project makes accurate 7-day and 28-day strength predictions important nowadays. Predicting slump and CS for 7 and 28 days was the main goal of this study. Using the collected data, MLR and ANN models were built. Various combinations of data division were used to achieve the highest level of accuracy for scatter plots used for qualitative analysis, as well as correlation coefficients and error measures. Models for slump, 7-day CS, and 28-day CS were built using divisions of the data in the percentages of 60%–40%, 70%–30%, 75%–25%, and 80%–20%. After all the testing, it was found that a data division of 80% -20 % (training–testing) provided the highest preciseness for both MLR and ELM in all the concrete grades mentioned. The data distribution to the training and testing models was kept constant in both models. This was done to compare how well the models operated on similar terrain. The developed models were tested on the remaining 20% of unseen values for slump prediction, 7-day CS, and 28-day tensile strength. The correlation coefficient, typically from 0.60 to 0.80, has shown that the MLR model predicts values with less accuracy. The fact that MLR can have difficulty understanding the non-linear relationship causes low correlation and significant errors.

Table 5. Comparison of MLR and ELM model results for 7 and 28-day CS.

Models	7 Days Compressive Strength			28 Days Compressive Strength		
	R^2	RMSE	MAE	R^2	RMSE	MAE
MLR	0.98	1.88	0.58	0.97	1.34	1.67
ELM	0.97	0.65	0.76	0.98	0.55	0.15

Table 5 compares two models of rubberized concrete in 7 and 28 days. MLR and ELM's performance in estimating the concrete's CS was compared. The results indicated that ELM performed better than MLR, as evidenced by higher R^2 values, lower RMSE and MAE values for both 7-day and 28-day predictions. For the 7-day predictions, ELM had a R^2 value of 0.97, RMSE of 0.65, and MAE of 0.76, while MLR had a R^2 value of 0.98, RMSE of 1.88, and MAE of 0.58. For the 28-day predictions, ELM had a R^2 value of 0.98, RMSE of 0.55, and MAE of 0.15, while MLR had a R^2 value of 0.97, RMSE of 1.34, and MAE of 1.67. These results indicate that ELM provides more accurate CS predictions than MLR. A comparison was made between two models, ELM and MLR, to determine their performance in terms of four key metrics: R^2, RSD, MRE, and running time. It was noted that R^2 it is a statistical measure representing the proportion of variance in the dependent variable that is predictable from the independent variable. It ranges from 0 to 1, with higher values indicating a better fit of the model. The best performance for R^2 is 1, showing that the model perfectly predicts the dependent variable. Root mean squared error measures the difference between the predicted and observed values, considering the discrepancy of all values. The smaller the RMSE value, the better the model fits the data. RSD measures the variability of the predicted values, expressed as a percentage of the mean. A lower

RSD value indicates less variability and a better model fit. MRE is the average relative discrepancy between the observed and predicted values. A lower MRE value indicates a better model fit.

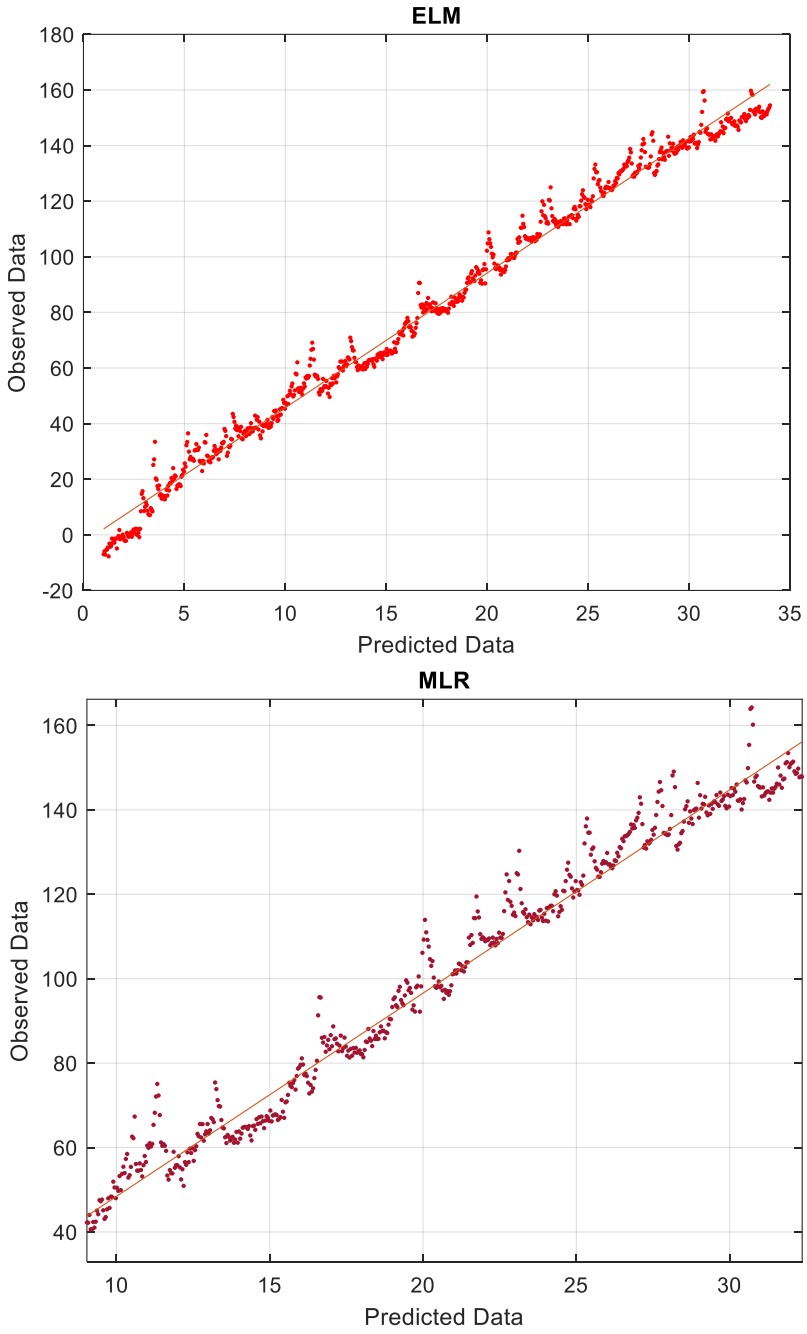

Fig. 6. Error noise in ELM and MLR.

Table 6. Performance values of two models.

Algorithm	R^2	RSD%	MRE%	Running Time/s
ELM	0.954	6.88	5.12	2.453
MLR	0.943	5.45	5.87	28.011

Following *Table 6*, the R^2 value measures the goodness of fit between the model and the data, with a value of 1 indicating a perfect fit. ELMs had a slightly higher R^2 value compared to MLR, with 0.954 compared to 0.943 for MLR. This suggests that ELM is a better fit for the data than MLR. The RSD value measures the RSD of the residuals and indicates how well the model predicts the data. ELMs had a higher RSD value than

MLR, with 6.88% compared to 5.45% for MLR. This suggests that ELM is less accurate in its predictions compared to MLR. The MRE value measures the MRE and indicates the average error in the model's predictions. ELM and MLR had similar MRE values, with 5.12% and 5.87%, respectively. This suggests that both models have similar levels of accuracy in their predictions. Looking at *Fig. 6*, the noise over the regression line in an ELM refers to the residual errors or deviations between the observed and predicted values. On the x-axis, the predicted data ranges from 0 to 35, while on the y-axis, the observed data ranges from -20 to 180. The noise in the ELM model is the difference between the predicted and observed values at each point along the regression line. The noise indicates that the model does not perfectly capture the relationship between the predictor and response variables. The magnitude and distribution of the noise over the regression line can provide valuable insights into the validity and accuracy of the model. Finally, the running time measures the time it takes for the model to complete its calculations. The ELM was significantly faster than MLR, with a running time of 2.45 seconds compared to 28.011 seconds for MLR. This suggests that ELM is a more efficient model compared to MLR. In conclusion, ELM provides slightly better performance in terms of R^2 compared to MLR, but has a slightly higher RSD value and similar MRE values. ELMs are also faster, providing more efficient calculations. Both models have their strengths and weaknesses, and the choice between them will depend on the specific requirements and constraints of the problem being solved.

4 | Conclusion

In predicting the CS, TS, and BSs of rubberized concretes, this work used an MLR and ELM neural network. The architecture, methodology, and learning methods were explained based on feedforward and backpropagation techniques. Data from a mixed test for rubber fiber concrete was collected based on recently published articles. The following step involved using a dataset generated from the literature. An ELM and MLR rubber fiber concrete strength prediction model was developed using a data set and the MATLAB platform. This study analyzed the mechanical properties of rubber fiber concrete with 10%, 20%, and 30% replacement of fine aggregates with rubber particles. The concrete was prepared by mixing dry ingredients in a laboratory mixer and adding polycarboxylic acid superplasticizer, water, and polypropylene fiber. The mixture was cast into cube, cylinder, and beam specimens and cured under laboratory conditions. The CS of rubber fiber concrete was higher in comparison with traditional concrete, with an increase of approximately 27% for 0.9 kg/m^3 rubber particles. The BS was also higher, increasing approximately 8%. The tensile strength was lower, with a decrease of approximately 14%. The results suggest that smaller rubber particles contribute to higher strength in rubberized concrete. The comparison between ELM and MLR models showed that ELM performed better in predicting the CS of rubberized concrete, with higher R^2 values and lower RMSE and MAE values for both 7-day and 28-day predictions. ELM had a R^2 of 0.97 (7 days) and 0.98 (28 days), a RMSE of 0.65 (7 days) and 0.55 (28 days), and a MAE of 0.76 (7 days) and 0.15 (28 days). MLR had a R^2 of 0.98 (7-day) and 0.97 (28-day), a RMSE of 1.88 (7-day) and 1.34 (28-day), and a MAE of 0.58 (7-day) and 1.67 (28-day). These results indicate that ELM provides more accurate predictions than MLR.

Author Contributions

M.S. conducted the experiments and analyzed the data. M.H. designed the study and provided supervision. E.T. and M.R. contributed to validation and manuscript preparation, and the final version was approved.

Funding

This study was conducted without external funding.

Data Availability

The data used in this study are available upon request from the corresponding author.

Conflict of Interest

The authors declare that they have no competing interests.

References

[1] Gencel, O., Kazmi, S. M. S., Munir, M. J., Kaplan, G., Bayraktar, O. Y., Yarar, D. O., … & Ahmad, M. R. (2021). Influence of bottom ash and polypropylene fibers on the physico-mechanical, durability and thermal performance of foam concrete: an experimental investigation. *Construction and building materials*, *306*, 124887. DOI:10.1016/j.conbuildmat.2021.124887

[2] Munir, M. J., Kazmi, S. M. S., Wu, Y. F., Patnaikuni, I., Wang, J., & Wang, Q. (2020). Development of a unified model to predict the axial stress–strain behavior of recycled aggregate concrete confined through spiral reinforcement. *Engineering structures*, *218*, 110851. DOI:10.1016/j.engstruct.2020.110851

[3] Munir, M. J., Kazmi, S. M. S., Khitab, A., & Hassan, M. (2016). *Utilization of rice husk ash to mitigate alkali silica reaction in concrete* [presentation]. Proceedings of 2nd international multi-disciplinary conference (Vol. 19, p. 20). University of Lahore, Gujrat Campus Pakistan. http://sites.uol.edu.pk/imdc2016/downloads/civil-engineering/Utilization of Rice Husk Ash to Mitigate Alkali Silica Reaction in Concrete.pdf

[4] Torretta, V., Rada, E. C., Ragazzi, M., Trulli, E., Istrate, I. A., & Cioca, L. I. (2015). Treatment and disposal of tyres: two EU approaches. A review. *Waste management*, *45*, 152–160. DOI:10.1016/j.wasman.2015.04.018

[5] Toghroli, A., Shariati, M., Sajedi, F., Ibrahim, Z., Koting, S., Mohamad, E. T., & Khorami, M. (2018). A review on pavement porous concrete using recycled waste materials. *Smart structures and systems*, *22*(4), 433–440. DOI:10.12989/sss.2018.22.4.433

[6] Shariati, M., Heirati, A., Zandi, Y., Laka, H., Toghroli, A., Kianmehr, P., … & Poi-Ngian, S. (2019). Application of waste tire rubber aggregate in porous concrete. *Smart structures and systems*, *24*(4), 553–566. DOI:10.12989/sss.2019.24.4.553

[7] Toghroli, A., Mehrabi, P., Shariati, M., Trung, N. T., Jahandari, S., & Rasekh, H. (2020). Evaluating the use of recycled concrete aggregate and pozzolanic additives in fiber-reinforced pervious concrete with industrial and recycled fibers. *Construction and building materials*, *252*, 118997. DOI:10.1016/j.conbuildmat.2020.118997

[8] Zabaniotou, A. A., Antoniou, N., & Stavropoulos, G. (2015). Novel sorbent materials for environmental remediation via depolymerization of used tyres. *Desalination and water treatment*, *56*(5), 1264–1273. DOI:10.1080/19443994.2014.953210

[9] Emiroglu, M., Yildiz, S., & Kelestemur, M. H. (2008). An investigation on ITZ microstructure of the concrete containing waste vehicle tire. *Computers and concrete*, 5(5), 503-508. https://doi.org/10.12989/cac.2008.5.5.503

[10] Asutkar, P., Shinde, S. B., & Patel, R. (2017). Study on the behaviour of rubber aggregates concrete beams using analytical approach. *Engineering science and technology, an international journal*, *20*(1), 151–159. DOI:10.1016/j.jestch.2016.07.007

[11] Youssf, O., Hassanli, R., & Mills, J. E. (2017). Mechanical performance of FRP-confined and unconfined crumb rubber concrete containing high rubber content. *Journal of building engineering*, *11*, 115–126. DOI:10.1016/j.jobe.2017.04.011

[12] Khatib, Z. K., & Bayomy, F. M. (1999). Rubberized portland cement concrete. *Journal of materials in civil engineering*, *11*(3), 206–213. DOI:10.1061/(asce)0899-1561(1999)11:3(206)

[13] Fedroff, D., Ahmad, S., & Savas, B. Z. (1996). Mechanical properties of concrete with ground waste tire rubber. *Transportation research record*, *1532*(1), 66–72. https://doi.org/10.1177/0361198196153200110

[14] Eldin, N. N., & Senouci, A. B. (1993). Rubber-tire particles as concrete aggregate. *Journal of materials in civil engineering*, *5*(4), 478–496. DOI:10.1061/(asce)0899-1561(1993)5:4(478)

[15] Hernández-Olivares, F., Barluenga, G., Bollati, M., & Witoszek, B. (2002). Static and dynamic behaviour of recycled tyre rubber-filled concrete. *Cement and concrete research*, *32*(10), 1587–1596. DOI:10.1016/S0008-8846(02)00833-5

[16] Shu, X., & Huang, B. (2014). Recycling of waste tire rubber in asphalt and portland cement concrete: an overview. *Construction and building materials*, *67*(Part B), 217–224. DOI:10.1016/j.conbuildmat.2013.11.027

[17] Al-Tayeb, M. M., Bakar, B. H. A., Ismail, H., & Akil, H. M. (2012). Impact resistance of concrete with partial replacements of sand and cement by waste rubber. *Polymer-plastics technology and engineering*, *51*(12), 1230–1236.

[18] Xue, J., & Shinozuka, M. (2013). Rubberized concrete: a green structural material with enhanced energy-dissipation capability. *Construction and building materials*, *42*, 196–204. DOI:10.1016/j.conbuildmat.2013.01.005

[19] Zheng, L., Huo, X. S., & Yuan, Y. (2008). Experimental investigation on dynamic properties of rubberized concrete. *Construction and building materials*, *22*(5), 939–947. https://doi.org/10.1016/j.conbuildmat.2007.03.005

[20] Pacheco-Torgal, F., Ding, Y., & Jalali, S. (2012). Properties and durability of concrete containing polymeric wastes (tyre rubber and polyethylene terephthalate bottles): an overview. *Construction and building materials*, *30*, 714–724. DOI:10.1016/j.conbuildmat.2011.11.047

[21] Tayeh, A. I. (2013). Effect of replacement of sand by waste fine crumb rubber on concrete beam subject to impact load: experiment and simulation. *Civil and environmental research*, *3*(13), 165–172.

[22] Zhu, X., Miao, C., Liu, J., & Hong, J. (2012). Influence of crumb rubber on frost resistance of concrete and effect mechanism. *Procedia engineering*, *27*, 206–213. DOI:10.1016/j.proeng.2011.12.445

[23] Ling, T. C. (2011). Prediction of density and compressive strength for rubberized concrete blocks. *Construction and building materials*, *25*(11), 4303–4306. DOI:10.1016/j.conbuildmat.2011.04.074

[24] Najim, K. B., & Hall, M. R. (2012). Mechanical and dynamic properties of self-compacting crumb rubber modified concrete. *Construction and building materials*, *27*(1), 521–530. DOI:10.1016/j.conbuildmat.2011.07.013

[25] Ismail, M. K., & Hassan, A. A. A. (2016). Performance of full-scale self-consolidating rubberized concrete beams in flexure. *ACI materials journal*, *113*(2), 207–218. DOI:10.14359/51688640

[26] Naderpour, H., & Mirrashid, M. (2018). An innovative approach for compressive strength estimation of mortars having calcium inosilicate minerals. *Journal of building engineering*, *19*, 205–215. DOI:10.1016/j.jobe.2018.05.012

[27] Saridemir, M. (2009). Prediction of compressive strength of concretes containing metakaolin and silica fume by artificial neural networks. *Advances in engineering software*, *40*(5), 350–355. DOI:10.1016/j.advengsoft.2008.05.002

[28] Sobhani, J., Najimi, M., Pourkhorshidi, A. R., & Parhizkar, T. (2010). Prediction of the compressive strength of no-slump concrete: a comparative study of regression, neural network and ANFIS models. *Construction and building materials*, *24*(5), 709–718. DOI:10.1016/j.conbuildmat.2009.10.037

[29] Ince, R. (2004). Prediction of fracture parameters of concrete by artificial neural networks. *Engineering fracture mechanics*, *71*(15), 2143–2159. DOI:10.1016/j.engfracmech.2003.12.004

[30] Abu Yaman, M., Abd Elaty, M., & Taman, M. (2017). Predicting the ingredients of self compacting concrete using artificial neural network. *Alexandria engineering journal*, *56*(4), 523–532. DOI:10.1016/j.aej.2017.04.007

[31] Uysal, M., & Tanyildizi, H. (2011). Predicting the core compressive strength of self-compacting concrete (SCC) mixtures with mineral additives using artificial neural network. *Construction and building materials*, *25*(11), 4105–4111. DOI:10.1016/j.conbuildmat.2010.11.108

[32] Vakhshouri, B., & Nejadi, S. (2016). ANFIS application to predict the compressive strength of lightweight self-compacting concrete. *2016 future technologies conference (FTC)* (pp. 28–35). IEEE. https://ieeexplore.ieee.org/abstract/document/7821586

[33] Mashhadban, H., Kutanaei, S. S., & Sayarinejad, M. A. (2016). Prediction and modeling of mechanical properties in fiber reinforced self-compacting concrete using particle swarm optimization algorithm and artificial neural network. *Construction and building materials*, *119*, 277–287. DOI:10.1016/j.conbuildmat.2016.05.034

[34] Tu, T. Y., Chen, Y. Y., & Hwang, C. L. (2006). Properties of HPC with recycled aggregates. *Cement and concrete research*, *36*(5), 943–950. DOI:10.1016/j.cemconres.2005.11.022

[35] Khan, M. I. (2012). Predicting properties of High Performance Concrete containing composite cementitious materials using artificial neural networks. *Automation in construction*, *22*, 516–524. DOI:10.1016/j.autcon.2011.11.011

[36] Prasad, B. K. R., Eskandari, H., & Reddy, B. V. V. (2009). Prediction of compressive strength of SCC and HPC with high volume fly ash using ANN. *Construction and building materials*, *23*(1), 117–128. DOI:10.1016/j.conbuildmat.2008.01.014

[37] Bui, D. K., Nguyen, T., Chou, J. S., Nguyen-Xuan, H., & Ngo, T. D. (2018). A modified firefly algorithm-artificial neural network expert system for predicting compressive and tensile strength of high-performance concrete. *Construction and building materials*, *180*, 320–333. DOI:10.1016/j.conbuildmat.2018.05.201

[38] Khosravani, M. R., Nasiri, S., Anders, D., & Weinberg, K. (2019). Prediction of dynamic properties of ultra-high performance concrete by an artificial intelligence approach. *Advances in engineering software*, *127*, 51–58. DOI:10.1016/j.advengsoft.2018.10.002

[39] Öztaş, A., Pala, M., Özbay, E., Kanca, E., Çağlar, N., & Bhatti, M. A. (2006). Predicting the compressive strength and slump of high strength concrete using neural network. *Construction and building materials*, *20*(9), 769–775. DOI:10.1016/j.conbuildmat.2005.01.054

[40] Chithra, S., Kumar, S. R. R. S., Chinnaraju, K., & Alfin Ashmita, F. (2016). A comparative study on the compressive strength prediction models for High Performance Concrete containing nano silica and copper slag using regression analysis and artificial neural networks. *Construction and building materials*, *114*, 528–535. DOI:10.1016/j.conbuildmat.2016.03.214

[41] Hendi, A., Behravan, A., Mostofinejad, D., Moshtaghi, S. M., & Rezayi, K. (2017). Implementing ANN to minimize sewage systems concrete corrosion with glass beads substitution. *Construction and building materials*, *138*, 441–454. DOI:10.1016/j.conbuildmat.2017.02.034

[42] Hodhod, O., & Salama, G. A. (2013). Analysis of sulfate resistance in concrete based on artificial neural networks and USBR4908-modeling. *Ain shams engineering journal*, *4*(4), 651–660. DOI:10.1016/j.asej.2013.02.007

[43] Sadrmomtazi, A., Sobhani, J., & Mirgozar, M. A. (2013). Modeling compressive strength of EPS lightweight concrete using regression, neural network and ANFIS. *Construction and building materials*, *42*, 205–216. DOI:10.1016/j.conbuildmat.2013.01.016

[44] Bingöl, A. F., Tortum, A., & Gül, R. (2013). Neural networks analysis of compressive strength of lightweight concrete after high temperatures. *Materials and design*, *52*, 258–264. DOI:10.1016/j.matdes.2013.05.022

[45] Altun, F., Kişi, Ö., & Aydin, K. (2008). Predicting the compressive strength of steel fiber added lightweight concrete using neural network. *Computational materials science*, *42*(2), 259–265. DOI:10.1016/j.commatsci.2007.07.011

[46] Duan, P., Shui, Z., Chen, W., & Shen, C. (2013). Effects of metakaolin, silica fume and slag on pore structure, interfacial transition zone and compressive strength of concrete. *Construction and building materials*, *44*, 1–6. DOI:10.1016/j.conbuildmat.2013.02.075

[47] Deng, F., He, Y., Zhou, S., Yu, Y., Cheng, H., & Wu, X. (2018). Compressive strength prediction of recycled concrete based on deep learning. *Construction and building materials*, *175*, 562–569. DOI:10.1016/j.conbuildmat.2018.04.169

[48] Abambres, M., & Lantsoght, E. O. L. (2019). ANN-based fatigue strength of concrete under compression. *Materials*, *12*(22), 3787. DOI:10.3390/ma12223787

[49] Getahun, M. A., Shitote, S. M., & Abiero Gariy, Z. C. (2018). Artificial neural network based modelling approach for strength prediction of concrete incorporating agricultural and construction wastes. *Construction and building materials*, *190*, 517–525. DOI:10.1016/j.conbuildmat.2018.09.097

[50] Dehghan, S., Sattari, G., Chehreh Chelgani, S., & Aliabadi, M. A. (2010). Prediction of uniaxial compressive strength and modulus of elasticity for Travertine samples using regression and artificial neural networks. *Mining science and technology*, *20*(1), 41–46. DOI:10.1016/S1674-5264(09)60158-7

[51] Faridmehr, I., Bedon, C., Huseien, G. F., Nikoo, M., & Baghban, M. H. (2021). Assessment of mechanical properties and structural morphology of alkali-activated mortars with industrial waste materials. *Sustainability (Switzerland)*, *13*(4), 1–25. DOI:10.3390/su13042062

[52] Shariati, M., Ramli Sulong, N. H., & Arabnejad Khanouki, M. M. (2010). *Experimental and analytical study on channel shear connectors in light weight aggregate concrete* [presentation]. Proceedings of the 4th international conference on steel composite structures (pp. 21–23). https://eprints.qut.edu.au/196792/

[53] Shariati, A., Sulong, N. H., Suhatril, M., & Shariati, M. (2012). Investigation of channel shear connectors for composite concrete and steel T-beam. *International journal of the physical sciences*, *7*(11), Article-number. DOI:10.5897/ijps11.1604

[54] Mohammadhassani, M., Nezamabadi-Pour, H., Suhatril, M., & Shariati, M. (2013). Identification of a suitable ANN architecture in predicting strain in tie section of concrete deep beams. *Structural engineering and mechanics*, *46*(6), 853–868. DOI:10.12989/sem.2013.46.6.853

[55] Toghroli, A., Mohammadhassani, M., Suhatril, M., Shariati, M., & Ibrahim, Z. (2014). Prediction of shear capacity of channel shear connectors using the ANFIS model. *Steel and composite structures*, *17*(5), 623–639. DOI:10.12989/scs.2014.17.5.623

[56] Paknahad, M., Shariati, M., Sedghi, Y., Bazzaz, M., & Khorami, M. (2018). Shear capacity equation for channel shear connectors in steel-concrete composite beams. *Steel and composite structures*, *28*(4), 483–494. DOI:10.12989/scs.2018.28.4.483

[57] Armaghani, D. J., Mirzaei, F., Shariati, M., Trung, N. T., Shariati, M., & Trnavac, D. (2020). Hybrid ann-based techniques in predicting cohesion of sandy-soil combined with fiber. *Geomechanics and engineering*, *20*(3), 191–205. DOI:10.12989/gae.2020.20.3.191

[58] Shariati, M., Mafipour, M. S., Mehrabi, P., Ahmadi, M., Wakil, K., Trung, N. T., & Toghroli, A. (2020). Prediction of concrete strength in presence of furnace slag and fly ash using Hybrid ANN-GA (artificial neural network-Genetic Algorithm). *Smart structures and systems*, *25*(2), 183–195. DOI:10.12989/sss.2020.25.2.183

[59] Mhaya, A. M., Fahim Huseien, G., Faridmehr, I., Razin Zainal Abidin, A., Alyousef, R., & Ismail, M. (2021). Evaluating mechanical properties and impact resistance of modified concrete containing ground Blast Furnace slag and discarded rubber tire crumbs. *Construction and building materials*, *295*, 123603. DOI:10.1016/j.conbuildmat.2021.123603

[60] Golafshani, E. M., & Behnood, A. (2021). Predicting the mechanical properties of sustainable concrete containing waste foundry sand using multi-objective ANN approach. *Construction and building materials*, *291*, 123314. DOI:10.1016/j.conbuildmat.2021.123314

[61] Alabduljabbar, H., Huseien, G. F., Sam, A. R. M., Alyouef, R., Algaifi, H. A., & Alaskar, A. (2020). Engineering properties of waste sawdust-based lightweight alkali-activated concrete: experimental assessment and numerical prediction. *Materials*, *13*(23), 1–30. DOI:10.3390/ma13235490

[62] Sadowski, Ł., Piechówka-Mielnik, M., Widziszowski, T., Gardynik, A., & Mackiewicz, S. (2019). Hybrid ultrasonic-neural prediction of the compressive strength of environmentally friendly concrete screeds with high volume of waste quartz mineral dust. *Journal of cleaner production*, *212*, 727–740. DOI:10.1016/j.jclepro.2018.12.059

[63] Ray, S., Haque, M., Ahmed, T., & Nahin, T. T. (2023). Comparison of artificial neural network (ANN) and response surface methodology (RSM) in predicting the compressive and splitting tensile strength of concrete prepared with glass waste and tin (Sn) can fiber. *Journal of king saud university-engineering sciences*, *35*(3), 185–199. https://doi.org/10.1016/j.jksues.2021.03.006

[64] Yeşilmen, S., & Tatar, B. (2022). Efficiency of convolutional neural networks (CNN) based image classification for monitoring construction related activities: a case study on aggregate mining for concrete production. *Case studies in construction materials*, *17*, e01372. DOI:10.1016/j.cscm.2022.e01372

[65] Almasaeid, H. H., Suleiman, A., & Alawneh, R. (2022). Assessment of high-temperature damaged concrete using non-destructive tests and artificial neural network modelling. *Case studies in construction materials*, *16*, e01080. DOI:10.1016/j.cscm.2022.e01080

[66] Toghroli, A., Shariati, M., Rehan, M., & Ibrahim, Z. (2017). *Investigation on composite polymer and silica fume rubber aggregate pervious concrete* [presentation]. Proceedings of the 5th international conference on advances in civil, structural and mechanical engineering-CSM (pp. 95–99). DOI: 10.15224/978-1-63248-132-0-56

[67] Li, D., Toghroli, A., Shariati, M., Sajedi, F., Bui, D. T., Kianmehr, P., … & Khorami, M. (2019). Application of polymer, silica-fume and crushed rubber in the production of Pervious concrete. *Smart structures and systems*, *23*(2), 207–214. DOI:10.12989/sss.2019.23.2.207

[68] Rajaei, S., Shoaei, P., Shariati, M., Ameri, F., Musaeei, H. R., Behforouz, B., & de Brito, J. (2021). Rubberized alkali-activated slag mortar reinforced with polypropylene fibres for application in lightweight thermal insulating materials. *Construction and building materials*, *270*. DOI:10.1016/j.conbuildmat.2020.121430

[69] Topçu, I. B., & Saridemir, M. (2008). Prediction of rubberized concrete properties using artificial neural network and fuzzy logic. *Construction and building materials*, *22*(4), 532–540. DOI:10.1016/j.conbuildmat.2006.11.007

[70] Bachir, R., Mohammed, A. M. S., & Habib, T. (2018). Using artificial neural networks approach to estimate compressive strength for rubberized concrete. *Periodica polytechnica civil engineering*, *62*(4), 858–865. DOI:10.3311/PPci.11928

[71] Jalal, M., Nassir, N., Jalal, H., & Arabali, P. (2019). On the strength and pulse velocity of rubberized concrete containing silica fume and zeolite: Prediction using multivariable regression models. *Construction and building materials*, *223*, 530–543. DOI:10.1016/j.conbuildmat.2019.06.233

[72] Jalal, M., Arabali, P., Grasley, Z., Bullard, J. W., & Jalal, H. (2020). Behavior assessment, regression analysis and support vector machine (SVM) modeling of waste tire rubberized concrete. *Journal of cleaner production*, *273*. DOI:10.1016/j.jclepro.2020.122960

[73] Cheng, M. Y., & Cao, M. T. (2016). Estimating strength of rubberized concrete using evolutionary multivariate adaptive regression splines. *Journal of civil engineering and management*, *22*(5), 711–720. DOI:10.3846/13923730.2014.897989

[74] Habib, A., & Yıldırım, U. (2021). Prediction of the dynamic properties in rubberized concrete. *Computers and concrete*, *27*(3), 185–197. DOI:10.12989/cac.2021.27.3.185

[75] David J. Olive. (2010). Multiple linear and 1D regression. *Southern illinois university, carbondale, united states*, 641. http://parker.ad.siu.edu/Olive/rrun.pdf

[76] Darwin, D., Dolan, C. W., & Nilson, A. H. (2016). *Design of concrete structures* (Vol. 2). McGraw-Hill Education New York, NY, USA:

[77] Harirchian, E., Kumari, V., Jadhav, K., Raj Das, R., Rasulzade, S., & Lahmer, T. (2020). A machine learning framework for assessing seismic hazard safety of reinforced concrete buildings. *Applied sciences*, *10*(20), 7153.

[78] Martínez-Álvarez, F., Schmutz, A., Asencio-Cortés, G., & Jacques, J. (2019). A novel hybrid algorithm to forecast functional time series based on pattern sequence similarity with application to electricity demand. *Energies*, *12*(1), 94. DOI:10.3390/en12010094

[79] Ahmad, M., Hu, J. L., Hadzima-Nyarko, M., Ahmad, F., Tang, X. W., Rahman, Z. U., … & Abrar, M. (2021). Rockburst hazard prediction in underground projects using two intelligent classification techniques: a comparative study. *Symmetry*, *13*(4), 632. DOI:10.3390/sym13040632

[80] Zhu, S., Lu, H., Ptak, M., Dai, J., & Ji, Q. (2020). Lake water-level fluctuation forecasting using machine learning models: a systematic review. *Environmental science and pollution research*, *27*(36), 44807–44819. DOI:10.1007/s11356-020-10917-7

[81] Naderpour, H., & Mirrashid, M. (2020). Proposed soft computing models for moment capacity prediction of reinforced concrete columns. *Soft computing*, *24*(15), 11715–11729. DOI:10.1007/s00500-019-04634-8

[82] Lin, C. J., & Wu, N. J. (2021). An ann model for predicting the compressive strength of concrete. *Applied sciences (Switzerland)*, *11*(9), 3798. DOI:10.3390/app11093798

[83] Ahmad, M., Hu, J. L., Ahmad, F., Tang, X. W., Amjad, M., Iqbal, M. J., … & Farooq, A. (2021). Supervised learning methods for modeling concrete compressive strength prediction at high temperature. *Materials*, *14*(8), 1983. DOI:10.3390/ma14081983

[84] Aalimahmoody, N., Bedon, C., Hasanzadeh-Inanlou, N., Hasanzade-Inallu, A., & Nikoo, M. (2021). Bat algorithm-based ann to predict the compressive strength of concrete—a comparative study. *Infrastructures*, *6*(6), 80. DOI:10.3390/infrastructures6060080

[85] Nikoo, M., Torabian Moghadam, F., & Sadowski, Ł. (2015). Prediction of concrete compressive strength by evolutionary artificial neural networks. *Advances in materials science and engineering*, *2015*. DOI:10.1155/2015/849126

[86] Hadzima-Nyarko, M., Nyarko, E. K., Ademović, N., Miličević, I., & Kalman Šipoš, T. (2019). Modelling the influence of waste rubber on compressive strength of concrete by artificial neural networks. *Materials*, *12*(4), 561. https://doi.org/10.3390/ma12040561

[87] Diaconescu, R. M., Barbuta, M., & Harja, M. (2013). Prediction of properties of polymer concrete composite with tire rubber using neural networks. *Materials science and engineering: B*, *178*(19), 1259–1267. DOI:10.1016/j.mseb.2013.01.014

[88] Abdollahzadeh, A., Masoudnia, R., & Aghababaei, S. (2011). Predict strength of rubberized concrete using atrificial neural network. *WSEAS transactions on computers*, *10*(2), 31–40.

[89] Nguyen, H., & Bui, X. N. (2019). Predicting blast-induced air overpressure: a robust artificial intelligence system based on artificial neural networks and random forest. *Natural resources research*, *28*(3), 893–907. DOI:10.1007/s11053-018-9424-1

[90] Ahmadi-Nedushan, B. (2012). An optimized instance based learning algorithm for estimation of compressive strength of concrete. *Engineering applications of artificial intelligence*, *25*(5), 1073–1081. DOI:10.1016/j.engappai.2012.01.012

[91] Chopra, P., Sharma, R. K., Kumar, M., & Chopra, T. (2018). Comparison of machine learning techniques for the prediction of compressive strength of concrete. *Advances in civil engineering*, *2018*. https://doi.org/10.1155/2018/5481705

[92] Huang, G. Bin, Chen, L., & Siew, C. K. (2006). Universal approximation using incremental constructive feedforward networks with random hidden nodes. *IEEE transactions on neural networks*, *17*(4), 879–892. DOI:10.1109/TNN.2006.875977

[93] Huang, G. B., Zhu, Q. Y., & Siew, C. K. (2006). Extreme learning machine: theory and applications. *Neurocomputing*, *70*(1–3), 489–501. https://doi.org/10.1016/j.neucom.2005.12.126

[94] Huang, G., Song, S., Gupta, J. N. D., & Wu, C. (2014). Semi-supervised and unsupervised extreme learning machines. *IEEE transactions on cybernetics*, *44*(12), 2405–2417. DOI:10.1109/TCYB.2014.2307349

[95] Huang, G. Bin, Zhou, H., Ding, X., & Zhang, R. (2012). Extreme learning machine for regression and multiclass classification. *IEEE transactions on systems, man, and cybernetics, part b: cybernetics*, *42*(2), 513–529. DOI:10.1109/TSMCB.2011.2168604

[96] Rong, H. J., Jia, Y. X., & Zhao, G. S. (2014). Aircraft recognition using modular extreme learning machine. *Neurocomputing*, *128*, 166–174. DOI:10.1016/j.neucom.2012.12.064

[97] Zong, W., & Huang, G. B. (2011). Face recognition based on extreme learning machine. *Neurocomputing*, *74*(16), 2541–2551. https://doi.org/10.1016/j.neucom.2010.12.041

[98] Liao, S., & Feng, C. (2014). Meta-ELM: ELM with ELM hidden nodes. *Neurocomputing*, *128*, 81–87. DOI:10.1016/j.neucom.2013.01.060

[99] Costa, L. A. L. F. d., Kunst, R., & de Freitas, E. P. (2022). Intelligent resource sharing to enable quality of service for network clients: the trade-off between accuracy and complexity. *Computing*, *104*(5), 1219–1231. DOI:10.1007/s00607-021-01042-5

[100] Janani, S., & Santhi, A. S. (2018). Multiple linear regression model for mechanical properties and impact resistance of concrete with fly ash and hooked-end steel fibers. *International journal of technology*, *9*(3), 526–536. DOI:10.14716/ijtech.v9i3.763